Measured Vehicular Antenna Performance

RAMON L. JESCH, SENIOR MEMBER, IEEE

Abstract—**Power gain radiation patterns of mobile antennas mounted in six different locations on a test vehicle were measured with and without typical lights and sirens mounted on the roof. The measurements were performed at frequencies representing the frequency bands of 25 to 50, 150 to 174, 400 to 512, and 806 to 866 MHz. In addition, special antennas consisting of three disguised antennas operating at discrete frequencies of 40.27, 162.475, and 416.975 MHz and one slot antenna operating at 413 MHz were also measured. Plots of power gain radiation patterns are given for the mobile antennas mounted in six different locations on the test vehicle and for the special antennas. Results showing the effects of poor grounding characteristics are also included. Recommended locations for mounting the mobile antennas are given for specific frequency bands.**

I. INTRODUCTION

LAW ENFORCEMENT and other public safety personnel utilize various types of communications and electronic equipment in the performance of their normal day-to-day activities. Every patrol car has a minimum of one mobile transceiver in the vehicle; often there is more than one unit installed in the vehicle. Moreover, law enforcement officials are concerned about the optimum positioning of the patrol car transceiver antenna to provide efficient and reliable communications. Positioning the antenna on the center of the car roof [1], [2] insures good radio transmission and reception in all directions and provides some protection against vandalism for unattended cars. Unfortunately, this location is also desirable for the patrol car lights and siren. Placing the lights and siren near the antenna degrades radio transmission and reception as does positioning the antenna on the car trunk or fender.

To determine the extent of this degradation, a program was undertaken by the National Bureau of Standards (NBS) Law Enforcement Standards Laboratory (LESL) to conduct tests with the antenna mounted in various locations on a vehicle, with and without typical lights and sirens mounted on the roof. Power gain radiation patterns [3] of the antenna were measured in various vehicle locations at frequencies representing the frequency bands of 25 to 50, 150 to 174, 400 to 512, and 806 to 866 MHz.

II. ANTENNAS AND MOUNTING LOCATIONS

A. Antennas

Base-loaded mobile antennas that operate in the frequency ranges of 36 to 42, 132 to 174, 450 to 470 MHz, plus a mobile gain antenna that operates in the 806 to 866 range, all of which are typical of those used by law enforcement agencies, were obtained for the power gain radiation pattern measurements. The antenna whips were cut to operate at discrete frequencies of 40, 150, 460, and 840 MHz, respectively. In addition, power gain radiation pattern measurements for three disguised antennas operating at discrete frequencies of 40.27, 162.475, and 416.975 MHz plus one slot antenna operating 413 MHz were also obtained.

B. Mounting Locations

Six locations were chosen to mount the mobile antennas on the test vehicle as shown in Fig. 1, three locations on the roof, two locations on the trunk and one location on the right-front fender. The test vehicle is a 1976 four-door sedan whose silhouette plus the roof and trunk area compare quite favorably with the late model vehicles used by law enforcement agencies. The vehicle dimensions and mounting locations are shown in Fig. 2.

III. MEASUREMENT APPROACH

A. Measurement System

Fig. 3 shows a block diagram of the test equipment and test vehicle located on a turntable at the test range where all the power gain radiation patterns were measured. A half-wave dipole antenna (vertically polarized) was substituted for the log periodic antenna for measurements in the 25–50 MHz frequency band. Software was developed to perform various calculations and manipulations of measurement data from the shaft encoder and spectrum analyzer and to plot polar displays of the antenna radiation patterns.

B. Power Gain of the Mobile Antenna

In preparation for the measurement of the power gain radiation patterns of the mobile antennas, standard reference level E-field conditions were established on the turntable at discrete frequencies of 40, 40.27, 150, 162.475, 413, 416.975, 460, and 840 MHz. Vertically polarized calibrated dipoles with the feedpoint at the same height as the test vehicle roof-top were placed in turn on the turntable to cover the above frequencies. A vertically polarized transmitting antenna at the same height was located approximately 53.4 m (175 ft) away from the center-point of the turntable (Fig. 3). At each frequency, the power level at the transmitting antenna (approximately 3 W) was recorded along with the spectral amplitude of the RF signal level received by the spectrum analyzer from the calibrated dipoles. Using the calibration curves for the dipoles, the electric field present at the test antenna location on the turntable at each of the discrete frequencies can be calculated. By substituting the test vehicle with the mobile antenna in place of the calibrated dipole on the turntable and duplicating the same power levels at the

Manuscript received November 1, 1984; revised April 8, 1985. This work was performed by the Law Enforcement Standards Laboratory of the National Bureau of Standards as part of the Technology Assessment Program of the National Institute of Justice.

The author is with the Electromagnetic Fields Division, National Bureau of Standards, Boulder, CO 80303. Telephone (303) 497-3496.

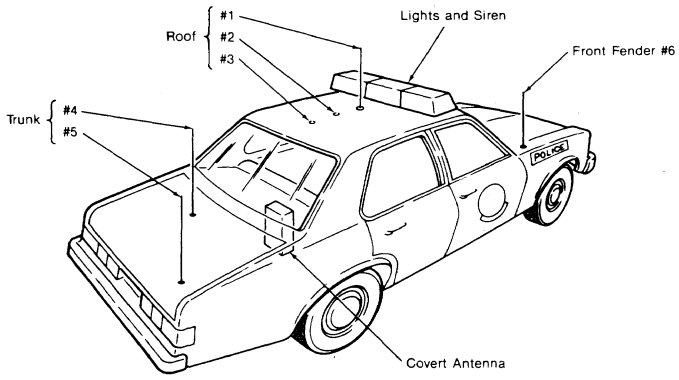

Fig. 1. Vehicle antenna location.

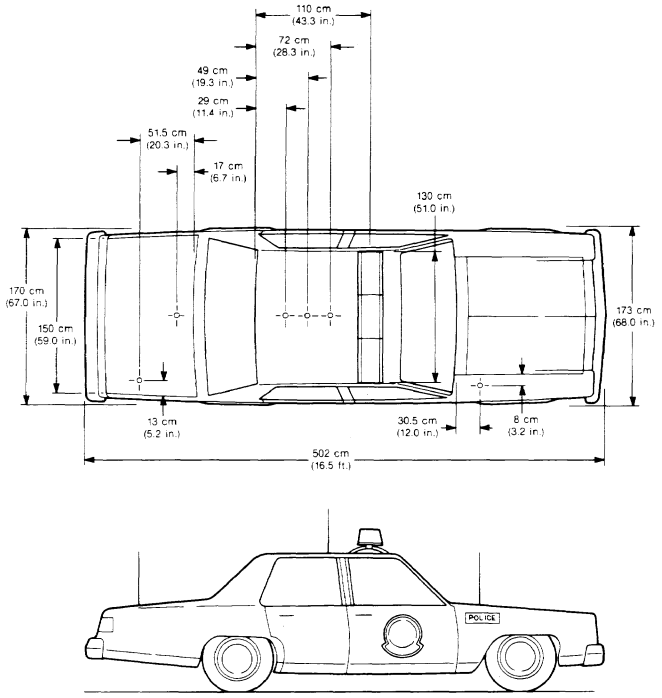

Fig. 2. Vehicle dimensions and mounting locations.

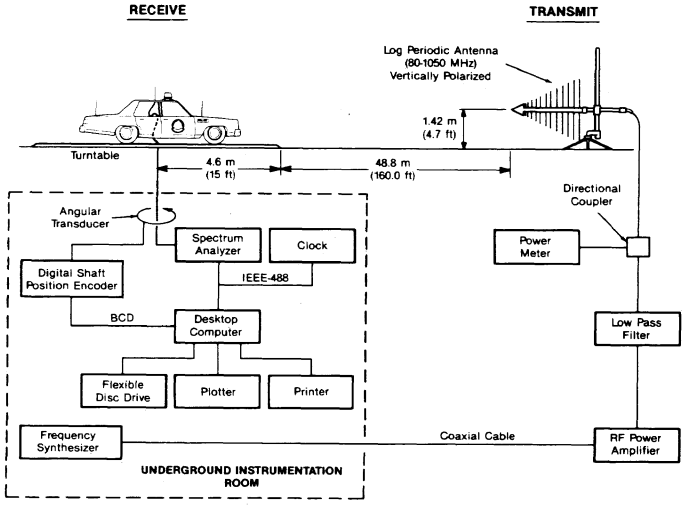

Fig. 3. Block diagram of measurement system.

transmitting antenna, the power gain of the mobile antenna can be obtained from the known electric field and the RF power level received at the mobile antenna by the following equation [4]:

$$G = 10 \log_{10} \left[W_r \frac{\eta_v}{E^2} \left(\frac{4\pi}{\lambda^2} \right) \right] \quad (1)$$

where

W_r power in watts received at the input to the test antenna as measured by the spectrum analyzer,
η_v $\sqrt{\mu_0/\epsilon_0} \approx 120\ \pi$ in ohms,
E electric field in volts per meter at the test antenna, and
λ the test frequency wavelength in meters.

This procedure enables absolute gain patterns to be obtained for each of the mobile antennas at each of the frequencies of interest and thereby allows antenna performance to be accurately compared from one antenna and location to another.

C. Power Gain Radiation Pattern Measurements

Power gain radiation patterns were measured for the mobile antennas operating at discrete frequencies of 40, 150, 460, and 840 MHz and in all six positions (Fig. 1) following the same test procedure described in Section III-B with and without lights and siren mounted on the test vehicle. The test vehicle was positioned directly over the center-point of the turntable for each location measured. By rotating the turntable, the radiation pattern representing the power gain at each angle in the azimuth plane was plotted on a polar display as a function of angular rotation. For each measurement run, approximately 300 to 400 data points were taken for one complete revolution of the turntable and used to plot the radiation pattern. In addition, three disguised antennas operating at discrete frequencies of 40.27, 162.47, and 416.915 MHz were measured only in one location on the right-front fender, i.e., the location where a regular AM radio antenna is normally mounted. Again, the power gain radiation pattern was measured with and without the lights and siren. Finally, one other antenna, a disguised 413 MHz slot antenna used in covert operations, was mounted in the trunk (Fig. 1) using the oval aperture normally used for a broadcast radio rear speaker. Once more, the power gain radiation pattern was measured with and without the lights and siren.

IV. MEASUREMENT RESULTS

Figs. 4–31 show plots of power gain radiation patterns as a function of the azimuth angle in degrees for each antenna measured at a designated frequency and mounting location; 0° is the front of the vehicle, 90° the right side, and 180° the rear. All radiation patterns are scaled to indicate absolute gain. All measurements were taken with and without the lights and siren mounted. Except as noted, all radiation patterns are plotted from data obtained when the lights and siren are mounted on the test vehicle.

The measurement uncertainty for the power gain measurements on the antennas was estimated at ±1 dB. All measurement data were corrected for cable and coupler losses plus the

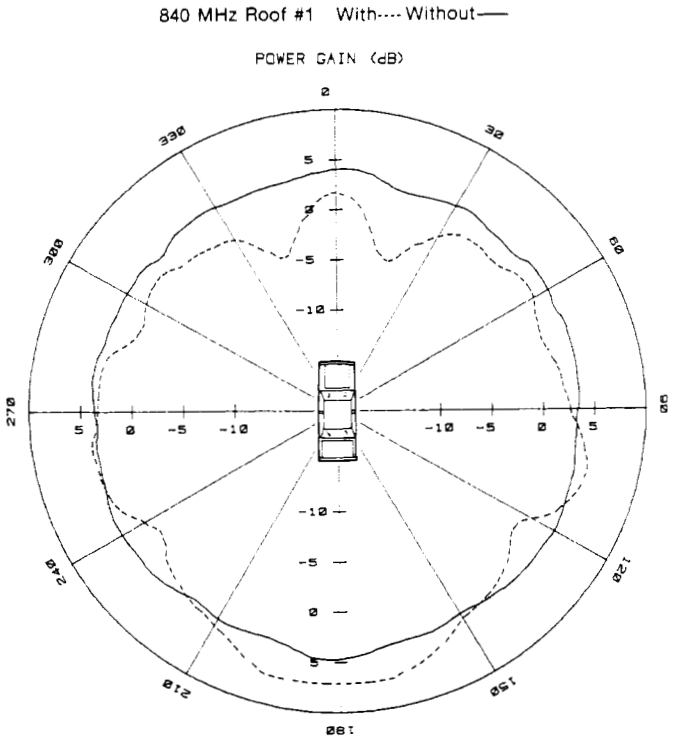

Fig. 4. Power gain radiation patterns of the 840 MHz mobile antenna measured at roof location 1 with and without lights and siren mounted.

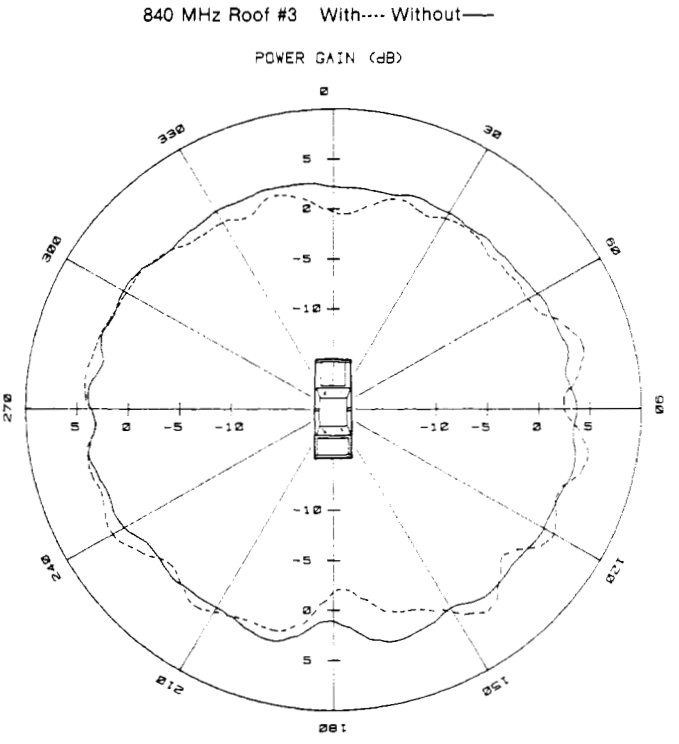

Fig. 6. Power gain radiation patterns of the 840 MHz mobile antenna measured at roof location 3 with and without lights and siren mounted.

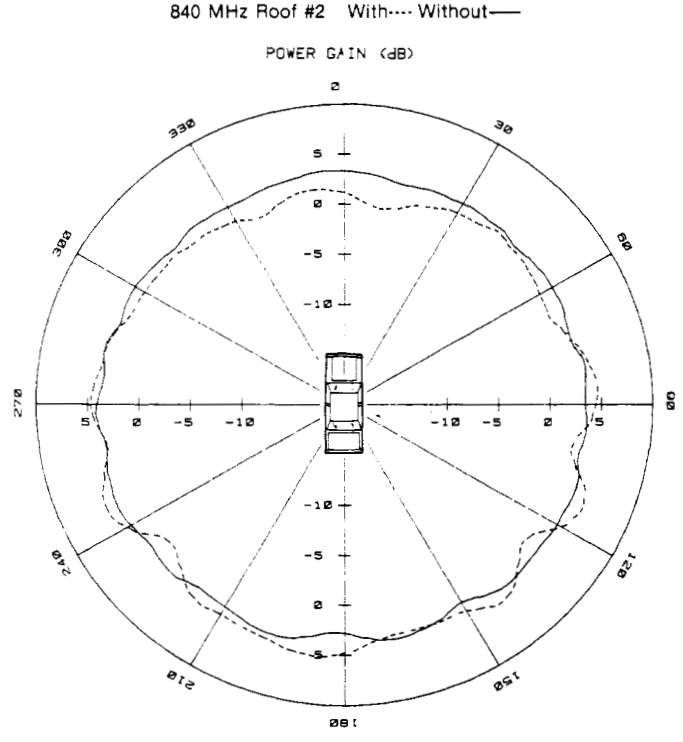

Fig. 5. Power gain radiation patterns of the 840 MHz mobile antenna measured at roof location 2 with and without lights and siren mounted.

calibration factors for the spectrum analyzer and the power meter.

A. 840 MHz Mobile Antennas

Figs. 4, 5, and 6 show plots of radiation patterns of the 840 MHz mobile gain antenna measured at roof locations 1, 2, and 3, respectively, with and without lights and siren mounted. Fig. 4 shows very clearly that placing the antenna near the lights and siren at location 1 distorts the radiation pattern. The gain of the antenna at this location with the lights and siren mounted varied from 7.1 dB maximum to −4.4 dB minimum while the gain of the antenna without the lights and siren mounted offered a more omnidirectional radiation pattern that varied from 4.8 dB maximum to 2.7 dB minimum. The radiation patterns measured in locations 2 and 3 are less affected by the lights and siren as shown in Figs. 5 and 6, respectively. Fig. 7 compares plots of the radiation patterns that were measured at roof mounting locations 1, 2, and 3 respectively with the lights and siren mounted. It is apparent that location 2 offers the best choice for this antenna on the roof at 840 MHz with lights and siren mounted. Even in this location, there still appears to be about a 2.5 dB transmission loss directly behind the lights and siren when compared with the plot without the lights and siren mounted.

Figs. 8, 9, and 10 show plots of the radiation patterns of the 840 MHz antenna measured at trunk locations 4 and 5 and location 6 on the right-front fender, respectively, with and without the lights and siren mounted. At these locations, the plots clearly show pattern distortion and several deep nulls. At location 4, the gain varied from 3.0 dB maximum to −11.4 dB minimum, while at location 5, the gain varied from 2.0 dB maximum to a particularly deep null of −49.0 dB, and at location 6, the gain varied from 3.7 dB maximum to −10.4 dB minimum all with the lights and siren mounted.

B. 460 MHz Mobile Antenna

Figs. 11, 12, and 13 show plots of radiation patterns of the 460 MHz base loaded mobile antenna measured at roof

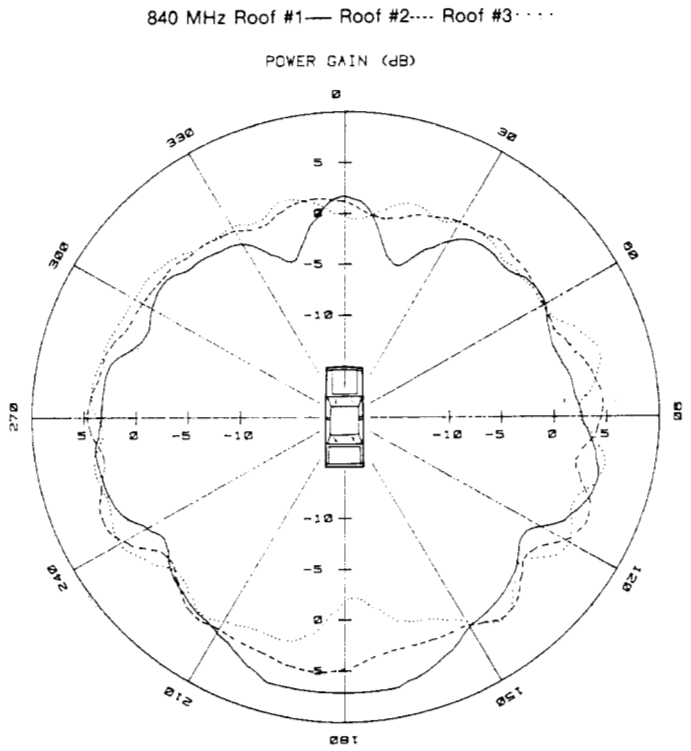

Fig. 7. Compares the 840 MHz power gain radiation patterns measured at roof locations 1, 2, and 3 with lights and siren mounted.

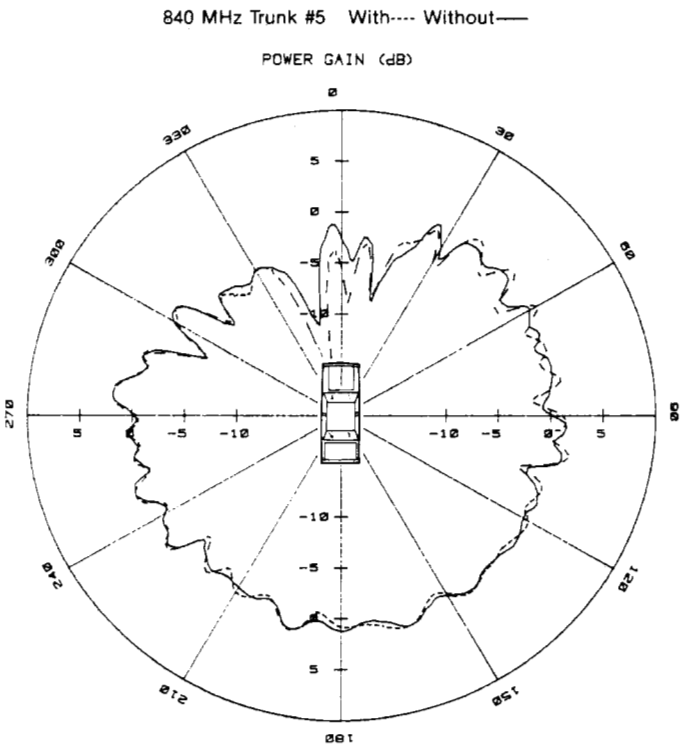

Fig. 9. Power gain radiation patterns of the 840 MHz mobile antenna measured at trunk location 5 with and without lights and siren mounted.

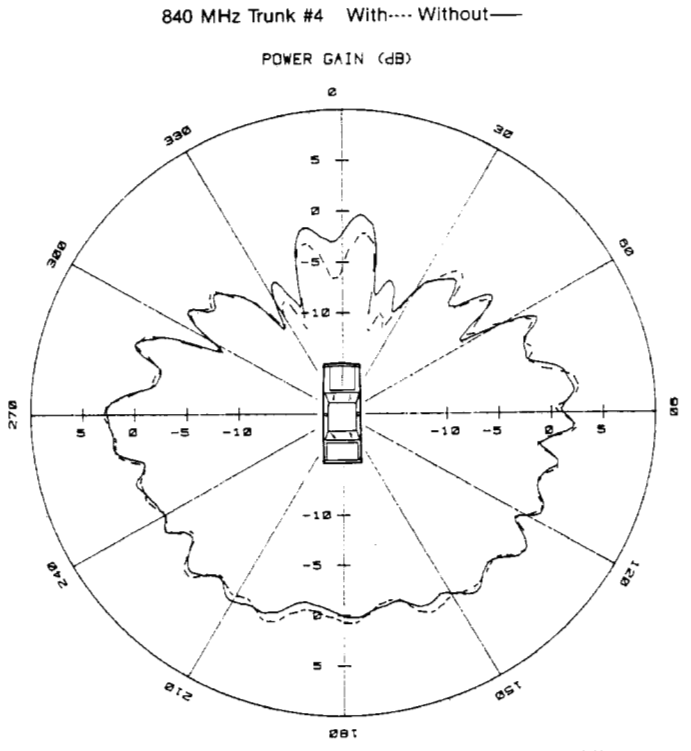

Fig. 8. Power gain radiation patterns of the 840 MHz mobile antenna measured at trunk location 4 with and without lights and siren mounted.

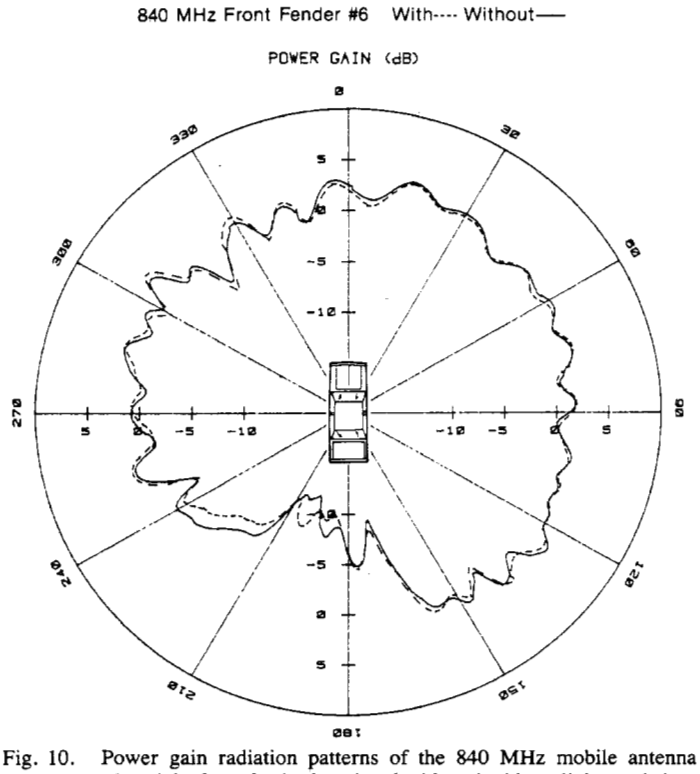

Fig. 10. Power gain radiation patterns of the 840 MHz mobile antenna measured at right-front fender location 6 with and without lights and siren mounted.

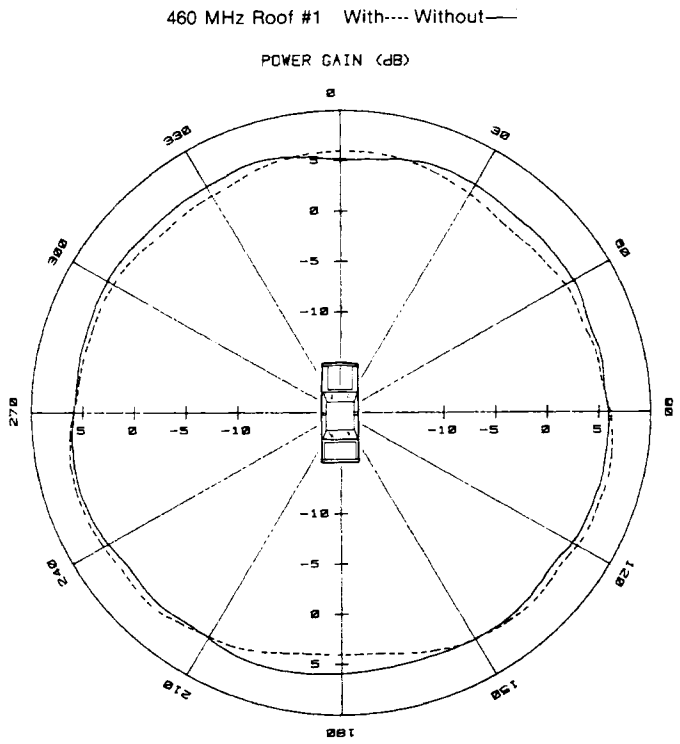

Fig. 11. Power gain radiation patterns of the 460 MHz mobile antenna measured at roof location 1 with and without lights and siren mounted.

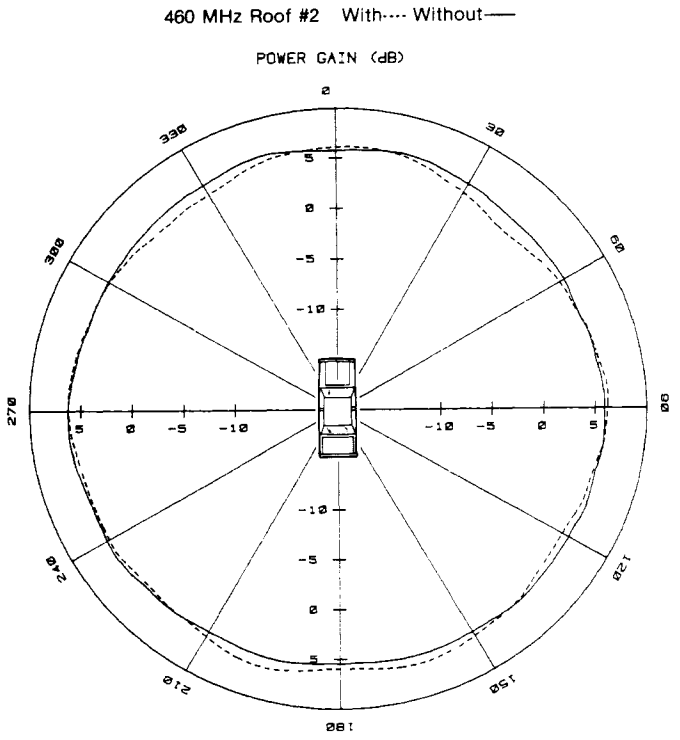

Fig. 12. Power gain radiation patterns of the 460 MHz mobile antenna measured at roof location 2 with and without lights and siren mounted.

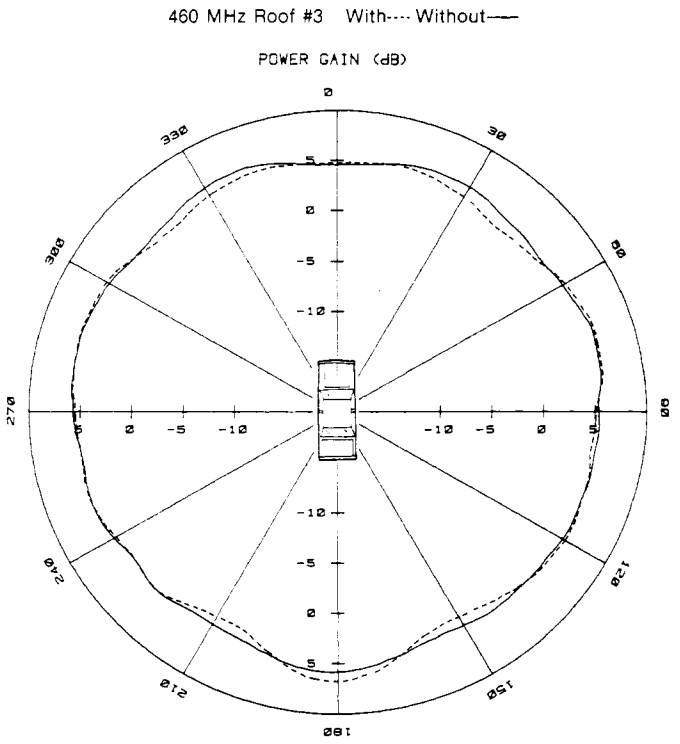

Fig. 13. Power gain radiation patterns of the 460 MHz mobile antenna measured at roof location 3 with and without lights and siren mounted.

locations 1, 2, and 3, respectively, with and without the lights and siren mounted. Already in this frequency band, there is less distortion of the radiation pattern due to the lights and siren. Figure 14 compares plots of the radiation patterns that were measured at roof mounting locations 1, 2, and 3, respectively, with the lights and siren mounted. Again, it appears that location 2 offers the best choice for locating this antenna on the roof at 460 MHz with lights and siren mounted. The maximum to minimum gain at this location varied from 6.8 dB to 3.9 dB, respectively.

Figs. 15, 16, and 17 show plots of the radiation patterns of the 460 MHz antenna measured at trunk locations 4 and 5 and location 6 on the right-front fender, respectively, with and without the lights and siren mounted. The pattern distortion is less at these locations than for the same locations at 840 MHz. At location 4, the gain varied from 5.2 dB maximum to -2.7 dB minimum, while at location 5, the gain varied from 4.7 dB maximum to -2.0 dB minimum, and at location 6, the gain varied from 5.7 dB maximum to -3.0 dB minimum all with the lights and siren mounted.

C. 150 MHz Mobile Antenna

Fig. 18 shows plots of radiation patterns of the 150 MHz base-loaded mobile antenna measured at roof location 1 with and without the lights and siren mounted. At this location, there is very little distortion of the radiation pattern due to the lights and siren which implies that similar plots for roof locations 2 and 3 need not be given. In any event, Fig. 19 contains the same information which compares plots of the radiation patterns that were measured at roof mounting locations 1, 2, and 3 with lights and siren mounted. Since there is little effect from the lights and siren distorting the radiation

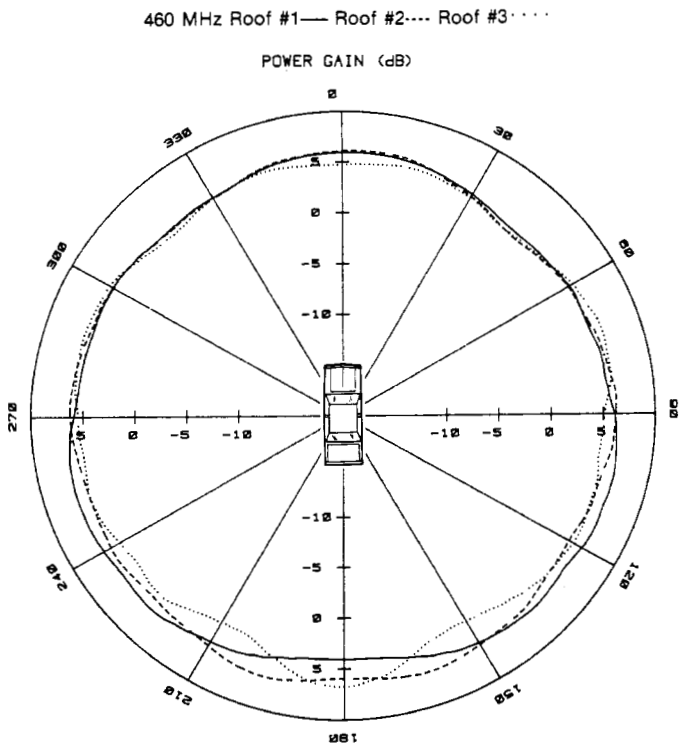

Fig. 14. Compares the 460 MHz power gain radiation patterns measured at roof locations 1, 2, and 3 with lights and siren mounted.

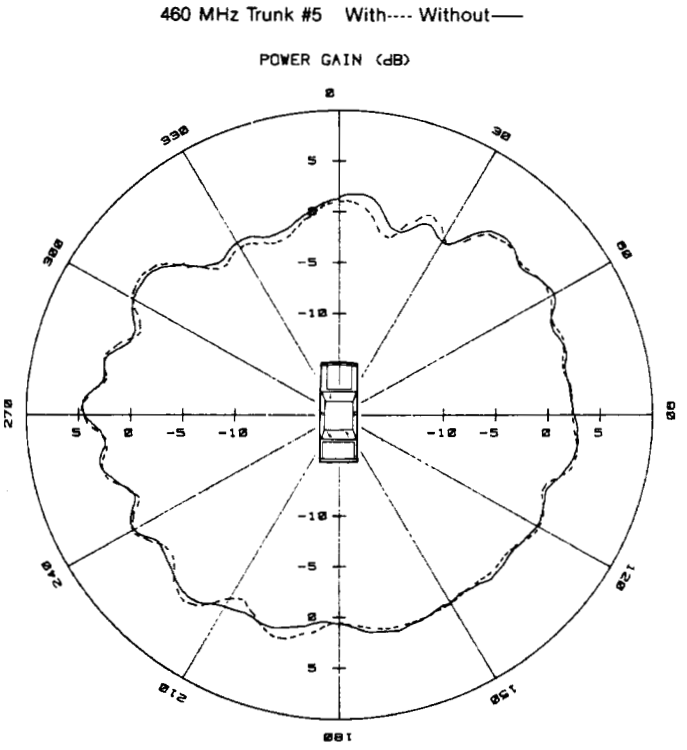

Fig. 16. Power gain radiation patterns of the 460 MHz mobile antenna measured at trunk location 5 with and without lights and siren mounted.

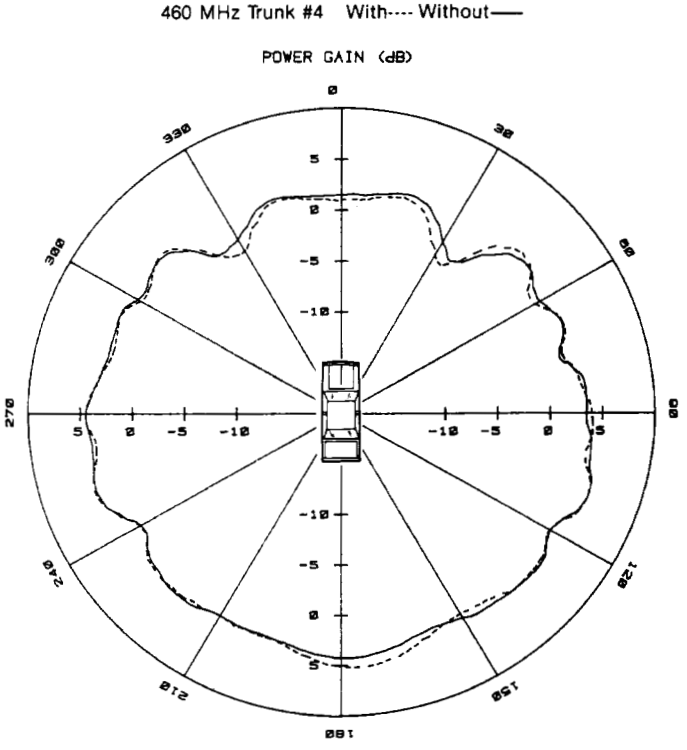

Fig. 15. Power gain radiation patterns of the 460 MHz mobile antenna measured at trunk location 4 with and without lights and siren mounted.

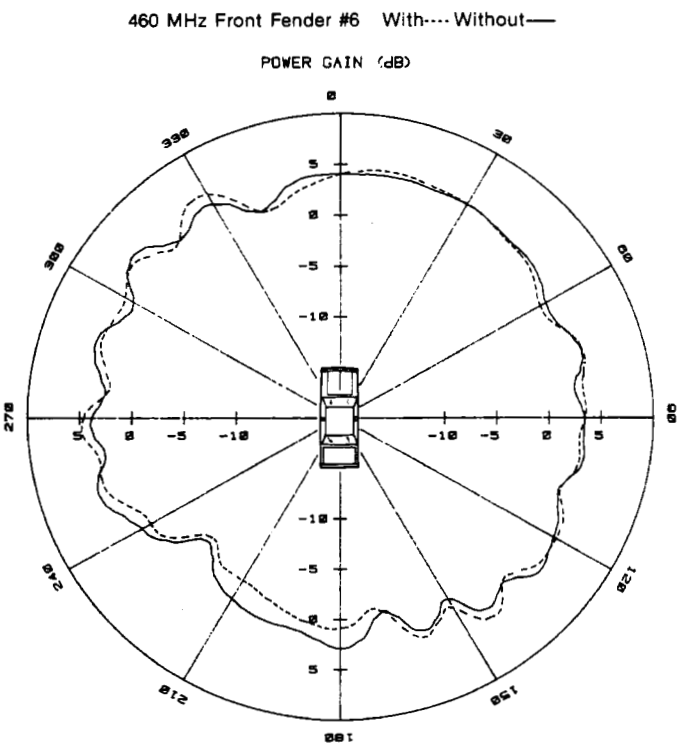

Fig. 17. Power gain radiation patterns of the 460 MHz mobile antenna measured at right-front fender location 6 with and without lights and siren mounted.

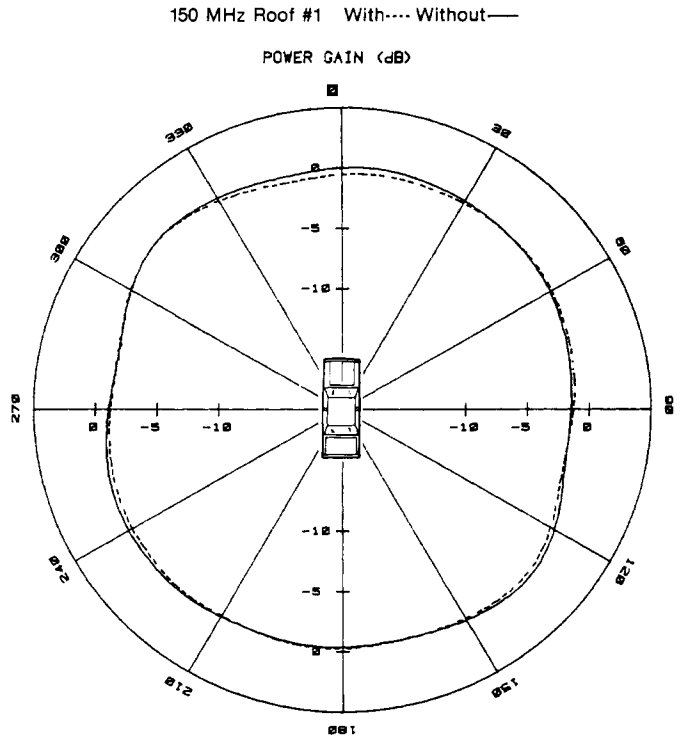

Fig. 18. Power gain radiation patterns of the 150 MHz mobile antenna measured at roof location 1 with and without lights and siren mounted.

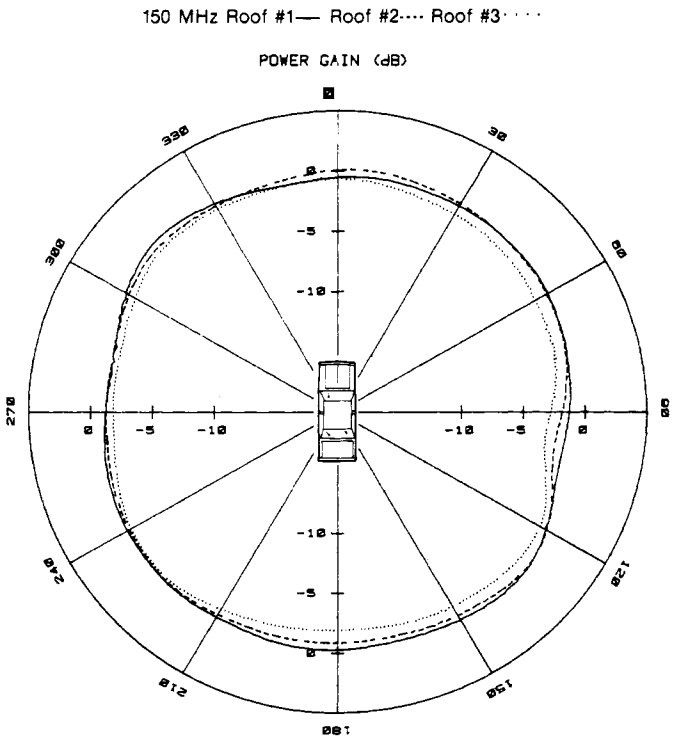

Fig. 19. Compares the 150 MHz power gain radiation patterns measured at roof locations 1, 2, and 3 with lights and siren mounted.

pattern, location 1 appears to offer a slightly better choice over location 2 for locating this antenna on the roof at 150 MHz with lights and siren mounted. The maximum to minimum gain at this location varied from 0.5 dB to −1.5 dB, respectively.

Fig. 20 compares the plots of the radiation patterns of the 150 MHz antenna that were measured at trunk locations 4 and 5 with the lights and siren mounted. For trunk location 4, the maximum to minimum gain varied from 0.1 dB to −2.2 dB, respectively, which could offer a good alternate choice of locations for mounting an antenna. Fig. 21 shows plots of the radiation patterns of the 150 MHz antenna that were measured at location 6 on the right-front fender with and without the lights and siren mounted. Both plots are given since this location shows more effect from the lights and siren distorting the radiation pattern.

D. 40 MHz Mobile Antenna

Fig. 22 shows plots of radiation patterns of the 40 MHz base loaded mobile antenna measured at roof location 1 with and without the lights and siren mounted. One can see that there is very little distortion of the radiation pattern due to the lights and siren. Fig. 23 compares plots of the radiation patterns that were measured at roof mounting locations 1, 2, and 3 with lights and siren mounted. Again, location 1 offers the best choice for locating this antenna on the roof at 40 MHz with lights and siren mounted. The maximum to minimum gain at this location varied from 0.2 dB to −1.8 dB, respectively.

Fig. 24 compares the plots of the radiation patterns of the 40 MHz antenna that were measured at trunk locations 4 and 5 with the lights and siren mounted. The radiation patterns are similar for both locations but not as omnidirectional as those at 150 MHz. Fig. 25 shows plots of power gain radiation patterns of the 40 MHz antenna that were measured at location 6 on the right-front fender with and without the lights and siren mounted.

E. Special Antennas

Figs. 26, 27, and 28 compare plots of the radiation patterns of three disguised antennas operating at discrete frequencies of 40.27, 162.475, and 416.975 MHz, respectively, with base-loaded mobile antenna counterparts operating at 40, 150, and 460 MHz, respectively. All measurements were taken at location 6 on the right-front fender with and without lights and siren mounted. Plots are given without lights and siren mounted. This location is of particular interest to those responsible for providing communications equipment for undercover vehicles.

Fig. 29 shows plots of radiation patterns of a 413 MHz slot antenna type used in covert operations that was mounted in the trunk using the oval aperture normally used for a broadcast radio rear speaker (Fig. 1). Measurements were taken with and without lights and siren mounted. The antenna exhibits an interesting radiation pattern which indicates a fairly good reception area on the rear of the vehicle. The two deep symmetrical nulls are characteristic of the slot antenna.

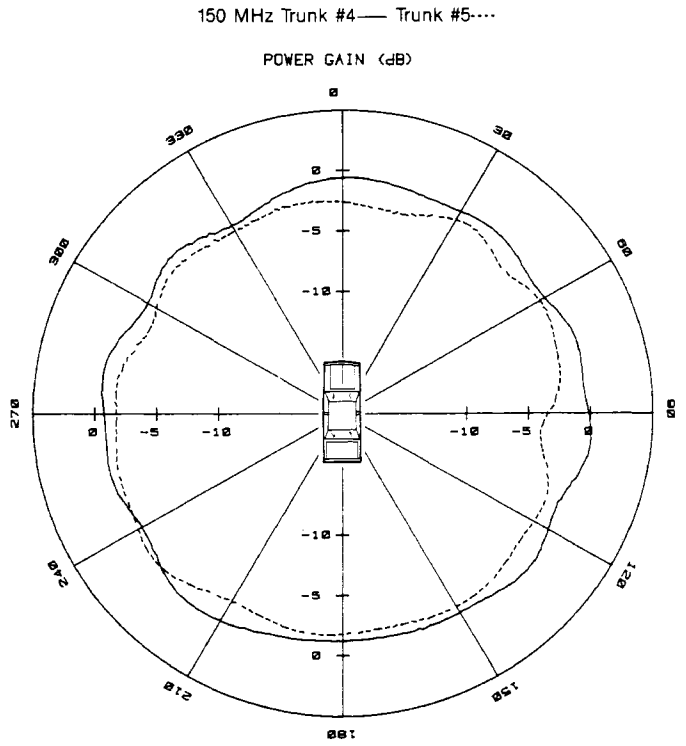

Fig. 20. Compares the 150 MHz power gain radiation patterns measured at trunk locations 4 and 5 with lights and siren mounted.

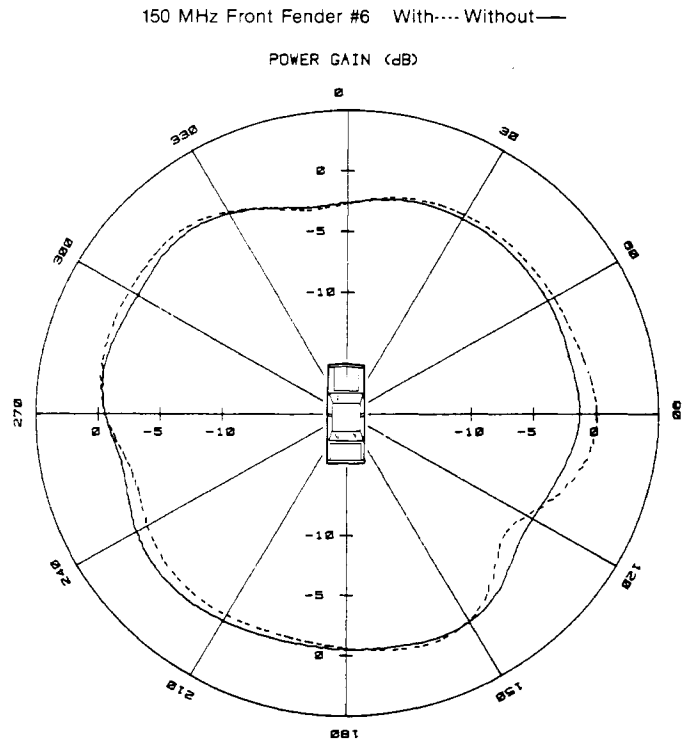

Fig. 21. Power gain radiation patterns of the 150 MHz mobile antenna measured at right-front fender location 6 with and without lights and siren mounted.

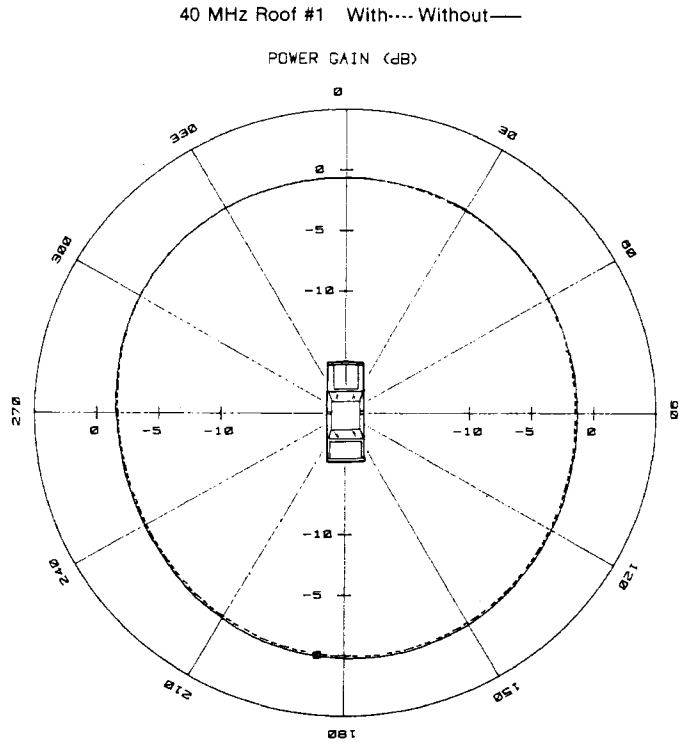

Fig. 22. Power gain radiation patterns of the 40 MHz mobile antenna measured at roof location 1 with and without lights and siren mounted.

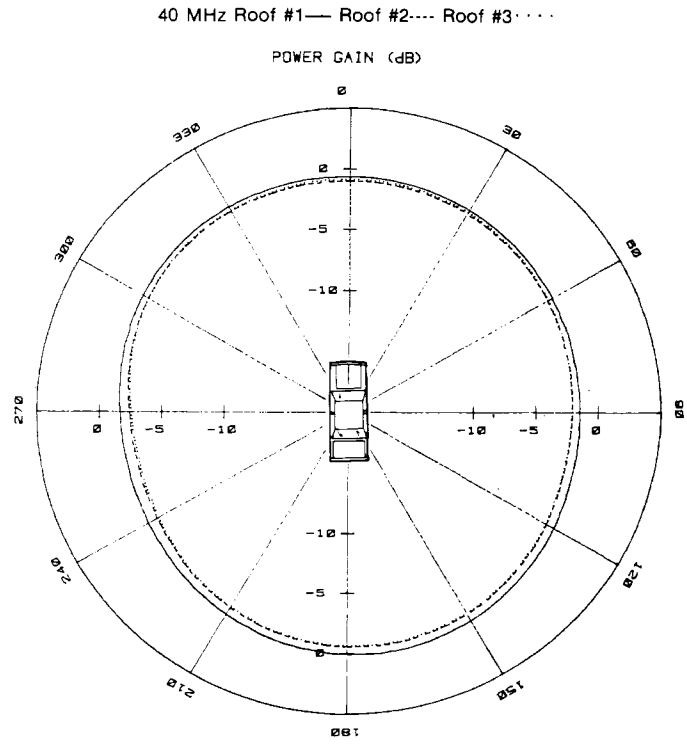

Fig. 23. Compares the 40 MHz power gain radiation patterns measured at roof locations 1, 2, and 3 with lights and siren mounted.

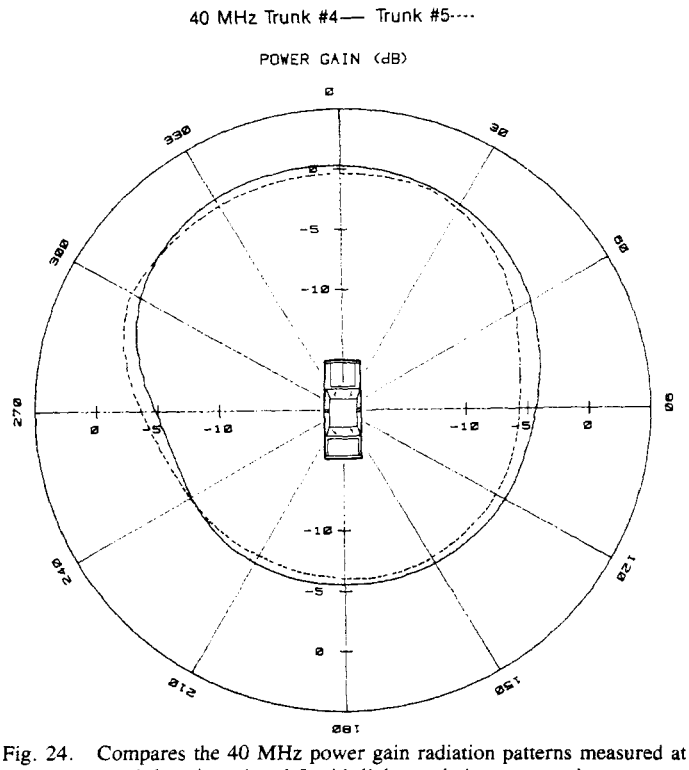

Fig. 24. Compares the 40 MHz power gain radiation patterns measured at trunk locations 4 and 5 with lights and siren mounted.

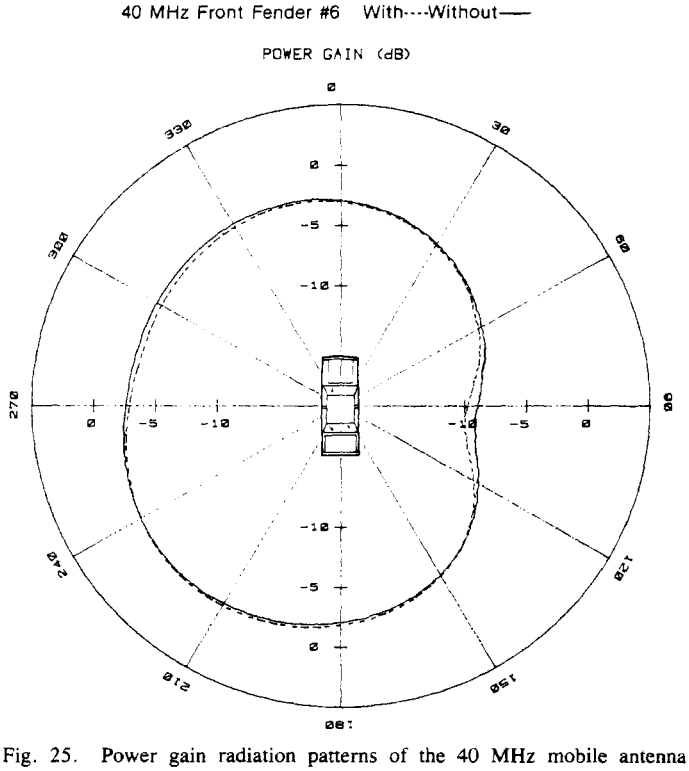

Fig. 25. Power gain radiation patterns of the 40 MHz mobile antenna measured at right-front fender location 6 with and without lights and siren mounted.

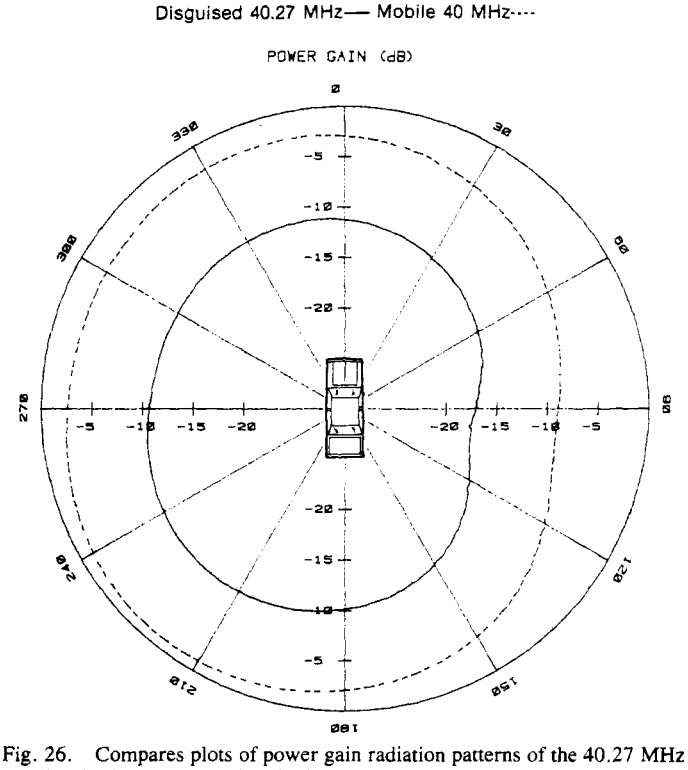

Fig. 26. Compares plots of power gain radiation patterns of the 40.27 MHz disguised antenna and the 40 MHz mobile antenna both measured at right-front fender location 6 without lights and siren mounted.

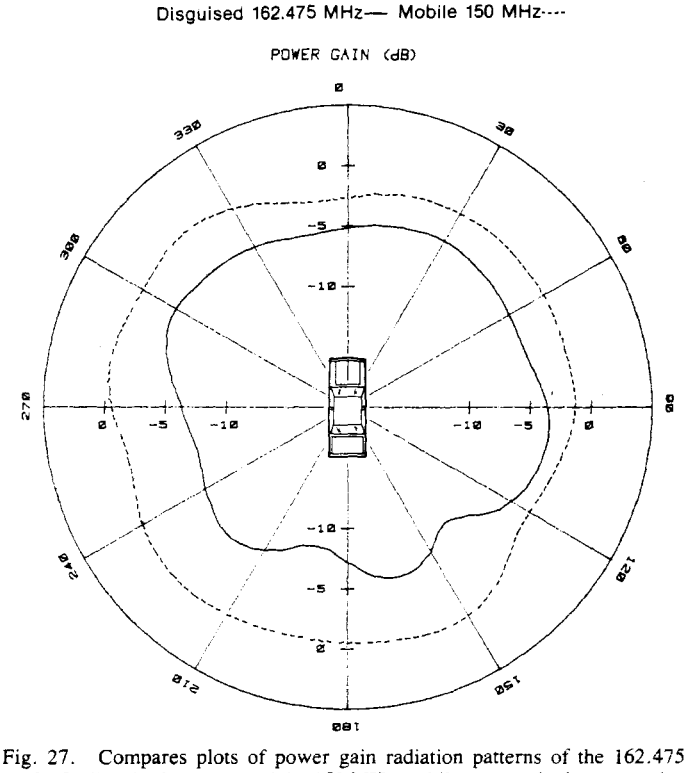

Fig. 27. Compares plots of power gain radiation patterns of the 162.475 MHz disguised antenna and the 150 MHz mobile antenna both measured at right-front fender location 6 without lights and siren mounted.

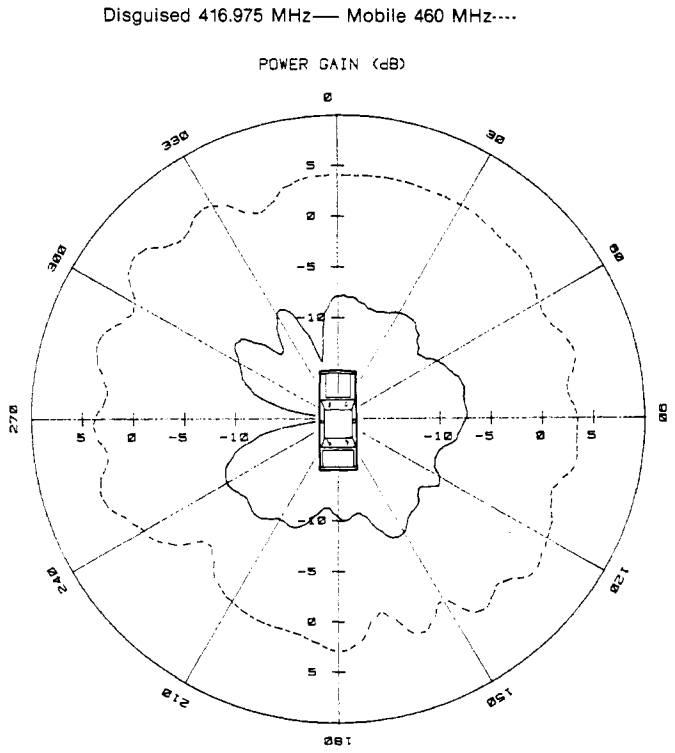

Fig. 28. Compares plots of power gain radiation patterns of the 416.975 MHz disguised antenna and the 460 MHz mobile antenna both measured at right-front fender location 6 without lights and siren mounted.

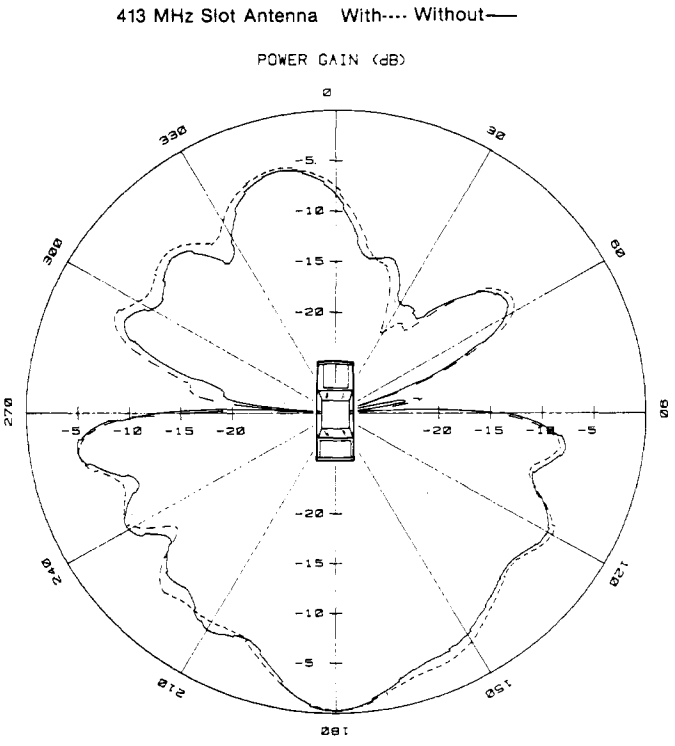

Fig. 29. Power gain radiation patterns of the 413 MHz slot antenna measured at the rear-speaker oval aperture with and without lights and siren mounted.

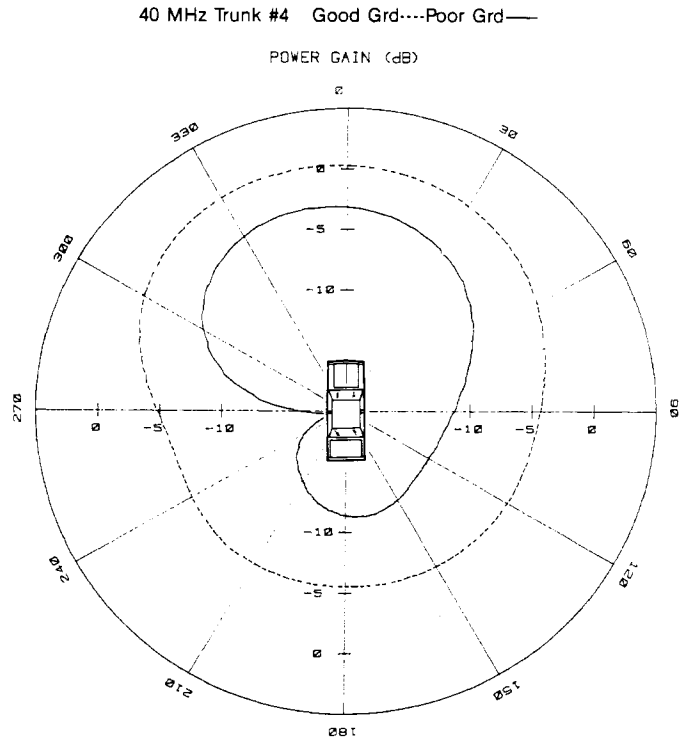

Fig. 30. Compares the 40 MHz power gain radiation patterns measured at trunk location 4 with and without a good ground of the trunk lid with lights and siren mounted.

F. Grounding Characteristics

Fig. 30 compares plots of the radiation patterns of the 40 MHz antenna measured at trunk location 4 with and without a good ground of the trunk lid to the rest of the vehicle with lights and siren mounted. A good ground connection was accomplished by taping several places on the trunk lid directly to the vehicle body by copper conducting tape. The solid curve in Fig. 30 is a plot of the radiation pattern of the mobile antenna without a good ground connection from the trunk lid to the vehicle body, while the dashed curve is a plot of the radiation pattern with a good ground. The power gain difference between the two plots varies between 3 dB and about 13 dB. Plots taken at location 5 also exhibited similar grounding characteristics.

Fig. 31 compares plots of the radiation patterns of the 40 MHz antenna measured at roof location 2 with and without a good ground connection of the lights and siren to the vehicle. The solid curve in Fig. 31 is a plot of the radiation pattern of the mobile antenna when the lights and siren were not properly grounded to the roof of the vehicle while the dashed curve is a plot of the radiation pattern with the lights and siren properly grounded to the roof of the vehicle. The plots show a difference of almost 2 dB when the lights and siren are not properly grounded to the vehicle.

V. SUMMARY AND CONCLUSION

Plots of power gain radiation patterns were obtained for specific mobile and special antennas at different frequencies and locations which allowed antenna performance to be accurately compared from one antenna and location to another. The measurements were performed at six different

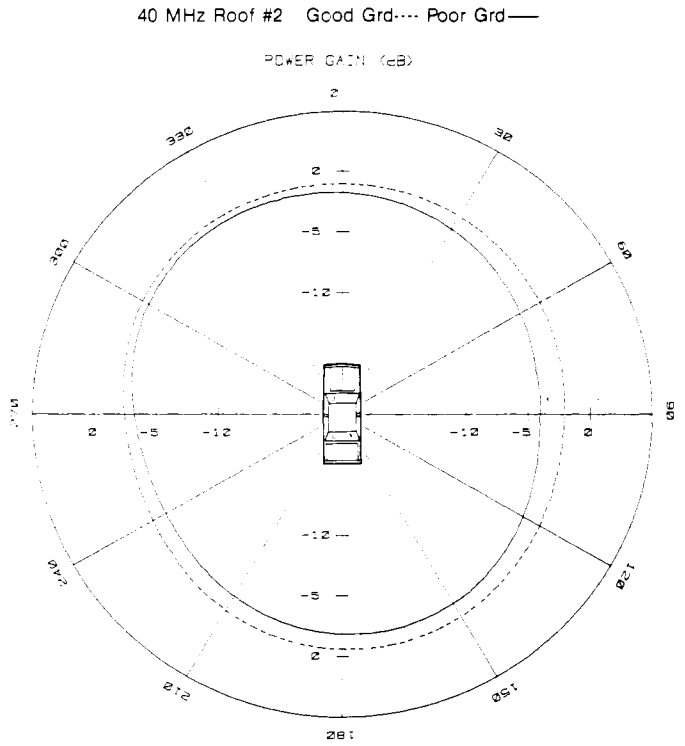

Fig. 31. Compares the 40 MHz power gain radiation patterns measured at roof location 2 with and without a good ground connection of the lights and siren to the vehicle.

locations on a 1976 four-door sedan, with and without typical lights and siren mounted on the roof. Note, if the same antennas were measured at similar locations on a smaller compact vehicle, the radiation patterns may not have been quite as uniform when compared with those from the larger vehicle because of the smaller ground plane [2]. Even though other types of mobile antennas may give some differences in radiation pattern and gain, the roof location gives the most nearly omnidirectional coverage since the vehicle roof provides a more uniform and symmetrical ground plane.

Out of the three roof locations, the best choice for mounting the mobile antennas used at 840 and 460 MHz was roof location 2 (Figs. 7 and 14) while the best choice for mounting the mobile antennas used at 150 and 40 MHz was roof location 1 (Figs. 19 and 23). Note at the two lower frequencies of 40 and 150 MHz, there was little distortion of the radiation pattern due to the lights and siren.

Among the nonroof locations, the best choice for mounting the mobile antennas was trunk location 4. At the higher frequencies of 840 and 460 MHz, there is distortion of the radiation pattern toward the front of the vehicle (Figs. 8 and 15) while at 150 and 40 MHz the radiation pattern was more nearly omnidirectional. Also, at 150 MHz, location 4 provides a good alternate location to the roof location.

The least recommended choice for mounting the mobile antennas is location 6 on the right-front fender where the data exhibited more pattern distortion than at the other recommended locations. However, this is an ideal location for mounting disguised antennas used in undercover vehicles to aid law enforcement personnel on surveillance.

In summary, the location of the antenna on the vehicle is critical to antenna performance. Further, the lights and sirens near the roof-mounted antenna did degrade antenna performance. Pattern distortion due to positioning the antenna on the car trunk or fender can now be readily determined from these power gain measurements. While proper grounding of the lights and siren plus providing an adequate ground plane on the trunk lid for the antennas was critical at 40 MHz, there only appeared to be little effect at 150 MHz and none at all above 400 MHz.

ACKNOWLEDGMENT

The author wishes to thank R. McLaughlin for his role in developing the computer software and measurement system; R. FitzGerrell for his recommendations regarding the technique used for measuring the absolute gain of vertically polarized mobile antennas; A. Wainwright for his help in making the measurements; and J. Monlux for her preparation of the manuscript.

REFERENCES

[1] D. W. Horn, "Vehicle-caused pattern distortion at 800 MHz," in *33rd IEEE Veh. Technol. Conf. Rec.*, May 1983, pp. 197-200.
[2] NIJ Rep. 202-83, "Mobile radio guide," pp. 16-21, Nov. 1983.
[3] IEEE Standard Test Procedures for antennas, IEEE Std. 149-1979 (Revision of IEEE Std. 149-1965), IEEE, New York, NY, 1979.
[4] E. C. Jordan, *Electromagnetic Waves and Radiating Systems*. Englewood Cliffs, NJ: Prentice-Hall, 1950, pp. 416-418.

Ramon L. Jesch (S'69-SM'84) was born in Beardsley, KS, on April 14, 1931. He received an A.A. degree from McCook College, McCook, NE, in 1956 and the B.S. degree in electrical engineering from the University of Colorado, Boulder, in 1959.

After graduation, he spent approximately two years with Martin-Denver in Systems Integration. In 1960 he joined the National Bureau of Standards in Boulder, CO, where he has been engaged in the development, evaluation and application of standards, instruments and techniques for measuring impedance, attenuation, phase, and properties of materials of transmission lines and other network structures. He is currently concerned with guiding technical research on problems in susceptibility and emission measurements for the evaluation of environmental electromagnetic fields and waves.

Mr. Jesch is a member of Phi Theta Kappa, Sigma Tau and Eta Kappa Nu. He serves as Deputy Technical Advisor of the USNC/IEC SC46D "Connectors for RF Cables."